# Evaluation of Leaf Heat Tolerance of Almond Germplasm in the UC Davis Almond Breeding Program

**Project No.:** **14-HORT21-Gilbert**

**Project Leader:** Matthew E. Gilbert
Department of Plant Sciences
UC Davis
One Shields Ave. Mail Stop 1
Davis, CA 95616
530.572.7846
megilbert@ucdavis.edu

**Project Cooperators and Personnel:**
Tom Gradziel and Nicolas Bambach, UC Davis
John Preece, USDA National Clonal Germplasm Repository, Davis
Craig Ledbetter, USDA ARS, Parlier

**Objectives:**

1. Establish a protocol for a high throughput tool for estimating leaf heat tolerance for future use.
2. Determine the quantitative impact that a high heat tolerance has on photosynthetic performance.
3. Provide ranking of leaf heat tolerance of 100 almond genotypes and related species used in the UC Davis Almond Breeding Program.
4. Evaluate if tradeoffs exist that prevent the incorporation of heat tolerance into commercial germplasm.

**Interpretive Summary:**

The Central Valley of California represents all that is good, and bad, for plant growth. The lack of summer rainfall leads to high light and productivities, but only provided that there is sufficient water for irrigation. The protected valley also has optimal daytime temperatures that can however be excessive for plants stressed by water deficits or salinity. Thus this new research project is focused on determining how, when and where heat stress affects almonds and the degree to which almonds varieties have different heat tolerance.

Almonds displayed two thresholds for heat effects on photosynthesis, one at leaf temperatures of 37 to 41$^{o}$C (99 to 106F) at which photosynthesis declines, but can recover, and the second starting at about 44$^{o}$C (111F) which is more severe (**Figure 1**). Note that these are leaf temperatures, not air temperatures. Almond leaves are generally cooler than the air, until severe water stress forces stomatal closure and loss of evaporative cooling, whereupon the leaves may be hotter than the air by 5 to even 10$^{o}$C. Thus almonds do not typically operate in the range of temperatures that would lead to heat stress, unless under additional water stress.

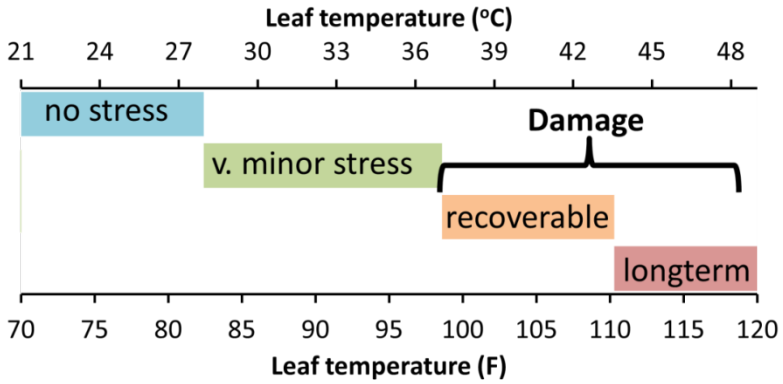


**Figure 1.** A semi-quantitative scale of heat stress effects on photosynthesis of almonds based upon measurements detailed in this report.

Monitoring of leaf performance in almonds demonstrated that heat stress occurred for leaves exposed to the combination of high air temperatures (~100F) and full sunlight and soil water deficit. However these leaves showed considerable ability to recover from the stress. It remains unclear how this stress and recovery quantitatively affects the photosynthetic performance of almonds in the field, but future work will provide some indication. From the point of view of growers, management that avoids plant water stress prior to, or on, days of excessive heat would be the only obvious way to avoid heat stress. It has been shown that kaolin application reduces leaf temperature and exposure to high light, and thus heat stress, but this is at the expense of long term photosynthesis (Rosati *et al.* 2006) thus it is unclear whether this is an option to prevent heat stress during periods of low irrigation.

A heat stress index was developed, and demonstrated that almonds at a range of representative sites in California, and the majority of years, would develop heat stress if they were also subject to water deficits or high salinity. However, all sites showed a two month period of low potential heat stress in April and May that could lead to acclimation prior to the high potential heat stress months of June to August. This aspect of almond heat tolerance remains to be tested.

A wide range of advanced almond breeding lines and new releases were evaluated for heat tolerance. Almond was shown to have a high heat tolerance relative to other species, and thus is not especially vulnerable to heat stress. Nor does it appear currently necessary to improve the heat tolerance of almond photosynthesis. However, it would be undesirable for almond breeding for traits such as self-compatibility to result in decreases in heat tolerance. Across 43 varieties of almonds including diverse sources of germplasm, there was very little variation in heat tolerance, being generally high. Thus it appears that breeding activities have not led to newly released varieties differing in leaf heat tolerance – an excellent sign.

## Materials and Methods:

Objective 1. Develop a protocol for high throughput measurement of leaf heat tolerance

A number of techniques are possible for the evaluation of leaf photosynthetic heat tolerance, including measuring $CO_2$ exchange and chlorophyll fluorescence. The former is technically difficult, while the latter have a number of different techniques possible (Knight *et al.* 2002; Cunningham *et al.* 2006). We chose to use that of Schreiber and Berry (1977) and Knight *et al*. (2002), in which a leaf is heated and photosynthetic function measured using a chlorophyll fluorometer that probes photosystem II (PSII). PSII is a the key component of photosynthesis responsible for absorption of 50% of the light that is used for photosynthesis, splitting of $O_2$ and the start of the electron transport chain necessary to fix $CO_2$ into photosynthetic products.

The apparatus that was developed for the protocol is described in **Figure 2** and a typical response of *Nonpareil* is shown in **Figure 3**. The advantages of this technique are:

1) Measurement of the entire temperature response on one leaf, rather than many leaves as in the maximal efficiency of PSII ($F_v/F_m$) technique of Cunningham and Read (2006). This successfully reduced variability.
2) Use of a leaf in a laboratory rather than in the field, rather than the need for large temperature variations and power requirements needed for field work.
3) Rapid measurements of a leaf in about 20 minutes; an increase of 1.5$^{o}$C per min.
4) The use of a simple heating system, rather than the considerable difficulty of heating a gas exchange system.

Protocol

1) During morning or cool afternoon, select a south west, south or south easterly facing, sunlit shoot from as high on the tree as possible, remove and immediately place in water. (Southerly shoots ensure that the shoots spend considerable time in the ambient conditions, and not in the shade.)
2) Place upright in shade in a double wall cardboard box with a tray of distilled water.
3) Return to laboratory without exceeding 85F and keeping shoots upright and with stem in water.
4) Acclimate overnight in distilled water in dark laboratory without direct sunlight, and dimmed overhead lights.
5) Select a young fully expanded leaf from the shoot, remove and place on cool heater plate.
6) Insert thermocouple thermometer under leaf, sandwiching a wet filter paper layer between the leaf and the heater. (The wet filter paper allows good thermal contact).
7) Place fluorometer holder on the leaf, and insert fluorometer fiberoptic.
8) Initiate measurements and start heating.
9) A line is fit to the fluorescence values below 32$^{o}$C and a second to values within 20% of the average fluorescence values of the transient. The intersection of the two linear fits is taken as the critical temperature at which the photosystem degrades.

In practice, up to twenty leaves can be analyzed per day, and all leaves should be measured within 3 days of harvest. Leaves did not change critical temperature threshold during this period.

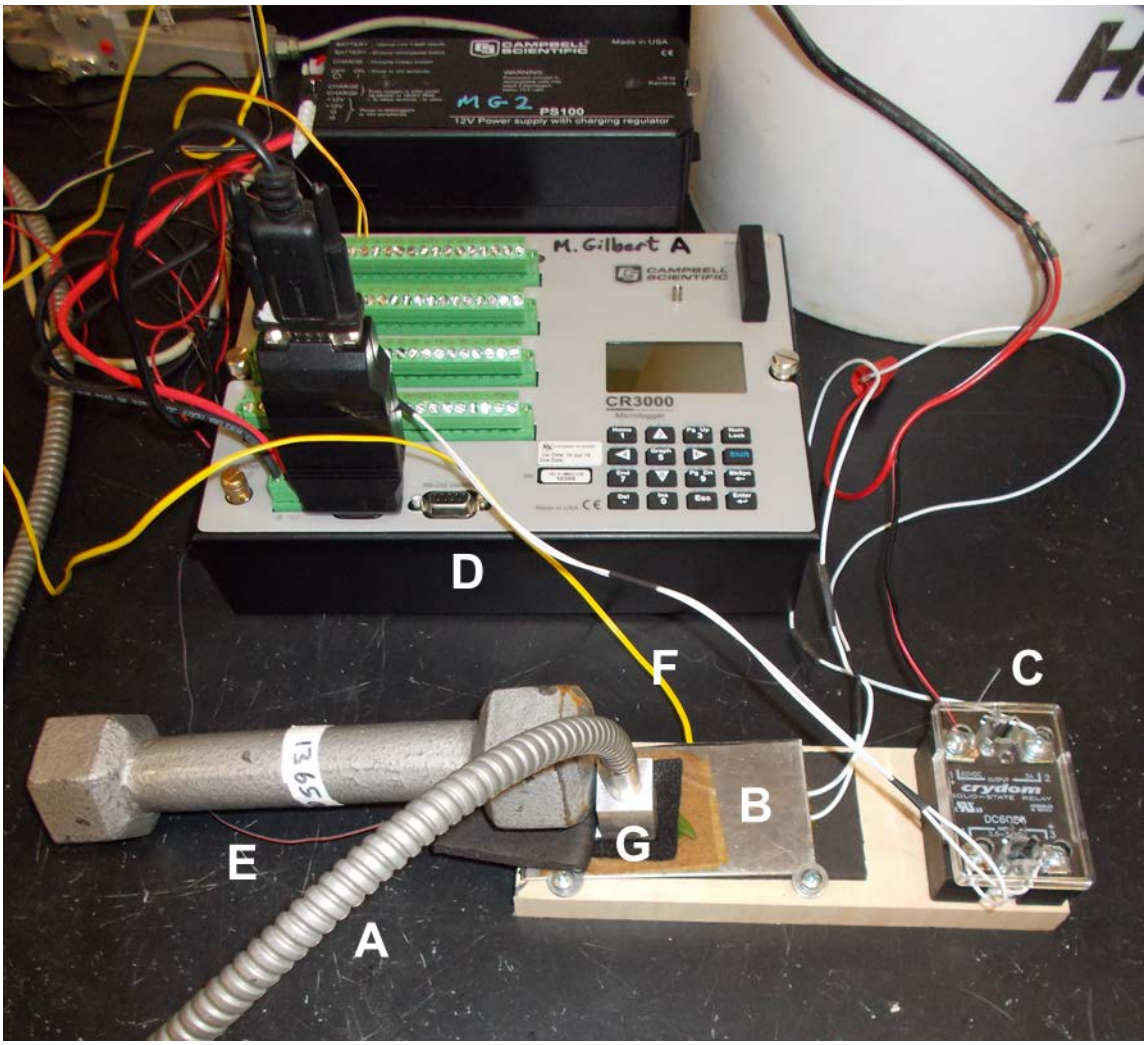


**Figure 2.** Apparatus developed to measure leaf heat tolerance, consisting of a Walz PAM2000 chlorophyll fluorometer (**A**) that measures photosynthetic function, a heater consisting of an aluminum sheet attached to a polyamide (kapton resistance 12V 15ohm) film heater (**B**), an electrical relay (**C**) allowing pulse width modulation (PWM) control of the heating rate using a precision datalogger (**D**). Leaf temperature was monitored using a 36 gauge E-type fine wire thermocouple (**E**) and the heater was controlled using a K-type 24 gauge thermocouple (**F**). An aluminum block (**G**) was drilled to allow a light tight holder of the fluorometer fiber optic, 9mm above the leaf surface. Condensation was prevented on the fluorometer via the high thermal conductance of the aluminum, and the milling of a groove in the block allowing venting of evaporated water.

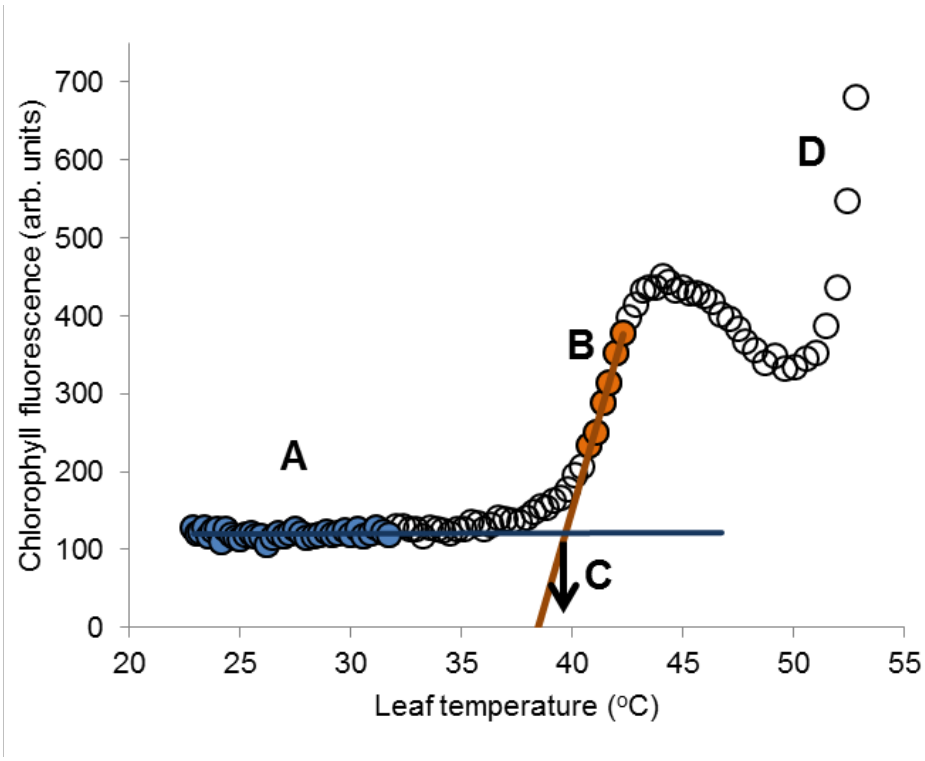


**Figure 3.** An example of thermal response of dark adapted chlorophyll fluorescence for a *Nonpareil* leaf taken during a 20min increase in temperature. Initially, fluorescence does not change with increasing temperature (**A**), while above a leaf temperature of ~40°C a rapid increase in fluorescence indicates increasing disorganization of the PSII photosynthetic apparatus (**B**). Interpolation of the two linear portions of the response provided a robust estimate of the critical leaf temperature at which photosynthetic damage occurred (**C**). At higher temperatures ~50°C cell damage results in more severe damage to the leaf (**D**).

Objective 2. What is the quantitative impact of high heat tolerance on leaf function?

Three approaches were developed to assess the quantitative impact of heat tolerance on leaf function:

1) Monitoring of potted almonds and orchard grown almonds for photosynthetic heat stress under drought conditions, with a rapid and slow imposition of drought, respectively.
2) Based upon the results from the field measurements, development and application of an index for the potential for heat stress in almonds exposed to large water deficits.
3) Development of a mechanistic photosynthesis model to determine the long term impact of heat stress on almonds.

*Objective 2a. Monitoring of almond heat stress*: Two experiments were undertaken in the summer of 2014, in which four Walz MonitoringPAM fluorometers were attached to leaves of five, one year old potted almonds (early summer) and subsequently (late summer) the same fluorometers were installed on mature almonds in the Student Orchard at the UC Davis Experimental Farm. The fluorometers also had light (PAR; photosynthetic active radiation), and temperature sensors attached to the leaves to allow them assess three components of heat and water stress. Pot experiments were conducted by monitoring two leaves prior to stress, and then imposition of water stress over two days, followed by five to seven days of recovery post irrigation, two leaves were also monitored on control, well-watered plants. The orchard experiment monitored two leaves on two trees with no irrigation starting in June and two leaves in two trees with full irrigation. Upper canopy leaves were accessed using a 9 foot metal

scaffold. For both experiments a leaf from each experiment was shaded using fine gauge stainless steel mesh (10 wires per cm) held at a distance of 30cm from the leaf. The pot experiment was done on *Nonpareil* almonds (*Nemaguard* rootstock) in 10 gallon pots, and fertigated regularly, and irrigated twice daily. The field experiment was done on two *Nonpareil* trees and two *Carmel* trees (one per irrigation treatment). Irrigation was withheld by removing microsprinklers at the treatment tree, and for the adjacent trees in the row and across the row. Natural variation in air temperature was used to impose heat stress treatments on different sets of leaves in the pot experiment.

As no photosynthetic differences were determined between the orchard and pot experiments, apart from rate of water deficit, the pot experiments were adopted for future work due to ease of measuring photosynthesis on short plants, and proximity to electrical outlets necessary for gas exchange measurements of photosynthesis. In June of 2015 16 potted two year old almonds, grown in 20 gallon pots, were installed at Orchard Park, UC Davis. These are currently being measured to provide more information on the heat tolerance of leaves of almonds.

*Objective 2b. Development of an index for heat stress*: The key conclusion from the work above was that three factors were necessary to lead the occurrence of heat stress in almonds; high air temperatures, high light conditions and closed stomata either due to high evaporative demands on hot days, salinity or soil water deficit. Based upon this information we developed the following index for heat stress that we used to assess the patterns of heat stress for six sites in California.

The index for heat stress is based upon a similar idea to the growing degree days concept. The index provides an indication of how many hours per day there was the potential for heat stress, *provided that a moderate to severe water deficit was present*, as was generally necessary for heat stress to negatively affect photosynthesis. The potential heat stress index (PHSI) is:

$$Potential\ Heat\ Stress\ Index = \ (PAR\ index) * [1 - (1 - T_{air}\ index) * (1 - VPD\ index)]$$

If applied to hourly weather data (e.g. from the CIMIS network) the PHSI has units of hours of potential heat stress, provided that a moderate to severe water deficit is present.

The PAR index is based upon almonds, and other crops, only using a limited portion of the total amount of light absorbed for photosynthesis, the rest is in excess, and has the potential to lead to leaf damage. Thus the PAR index is proportional to 1 minus the ratio of actual photosynthesis and the potential rate of photosynthesis if all light was used.

$$PAR\ index = 1 - \frac{actual\ photosynthesis}{potential\ photosynthesis}$$

Actual photosynthesis is modelled using a simplified equation from the published values of Rosati *et al*. (2006):

$$actual\ photosynthesis = \frac{pot.photo.+22.3-\sqrt{(pot.photo.+22.3)^2-3.568*pot.photo.}}{1.6}$$

And potential photosynthesis (pot. photo.) is:

$$pot.photo. = 0.05 * PAR$$

PAR is the photosynthetically active radiation (μmol $m^{-2}$ $s^{-1}$) and can be estimated as: PAR = 2*solar radiation (W $m^{-2}$ or J $m^{-2}$ $s^{-1}$) from CIMIS data.

The VPD index relates to stomatal closure when the vapor pressure deficit (VPD), a proxy for evaporative demand, is high. Almonds do not close stomata drastically under most environmental conditions, but based upon the data of Rosati *et al*. (2006) a VPD of 50% closure was assigned to a VPD of 5kPa, which corresponds with very hot air temperatures and low humidity. The VPD index was:

$$VPD\ index = 1-\frac{1}{1+3^{VPD-5}}$$

VPD was calculated from hourly CIMIS data using the following formula:

VPD=0.61365*exp((17.502*$T_{air}$)/(240.97+ $T_{air}$))-relative humidity(%)*0.61365*exp((17.502* $T_{air}$)/(240.97+ $T_{air}$))/100

Finally the $T_{air}$ index was based upon the thermal threshold for unrecoverable heat damage in the absence of light determined on leaves using almond the $F_v/F_m$ method of Cunningham and Read (2006). Note that this is a higher threshold than the critical leaf temperature used in Objective 3; the reason being that the $T_{air}$ index represents unrecoverable damage while the heat tolerances measured by critical leaf temperature in Objective 3 are potentially recoverable. The leaf temperature used in the calculation was based upon the assumption that 100 W $m^{-2}$ of solar radiation results in a 1$^{o}$C increase in leaf temperature above ambient, as was observed in the drought treatments in the initial experiments. This assumes that the leaf is *a moderate to severe water deficit* leading to stomatal closure and no evaporative cooling. Thus,

$$T_{air}\ index = 1-\frac{1}{1+1.54^{T_{air}+\frac{SolarRadiation}{100}-49.6}}$$

where 1.54 and 49.6$^{o}$C are the empirical fitted values representing the loss of $F_v/F_m$ with leaf heating in the dark (**Figure 8**).

**Table 1.** Typical values for the Potential Heat Stress Index (PHSI), Relative Humidity was 15%

| Conditions | Air temperature | Solar radiation | PHSI |
|---|---|---|---|
| Hot, high light | 40$^{o}$C (104F) | 900 W m$^{-2}$ | 0.68 hours |
| Warm, high light | 35$^{o}$C (95F) | 900 W m$^{-2}$ | 0.38 hours |
| Cool, high light | 30$^{o}$C (86F) | 900 W m$^{-2}$ | 0.14 hours |
| Hot, cloudy | 40 $^{o}$C (104F) | 250 W m$^{-2}$ | 0.29 hours |
| Cool, cloudy | 30 $^{o}$C (86F) | 250 W m$^{-2}$ | 0.06 hours |

The PHSI was applied to twenty years of hourly data obtained from CIMIS for six sites representing the northern, middle and southern Central Valley almond growing areas. The objective was to determine, when and where heat stress is likely to be an issue, in how many years and with what seasonality. For reference, **Table 1** illustrates PHSI values for a range of conditions typical of varying degress of stress. Here PHSI is highest for the combination of hot and sunny days.

*Objective 2c. Development of a model of photosynthetic heat stress*: This was done and partially validated using the experiments detailed in Objective 2a. The model is technical and is included in Appendix 1. The ongoing experiments in 2015 are designed to fully validate and test the model. The model will be applied to determine the long term quantitative impact of heat stress on almond photosynthetic performance.

Objective 3. Rank the heat tolerance of almond genotypes and related species

A conclusion from the application of the Potential Heat Stress Index modeling was that heat stress peaks in the middle summer and acclimation is likely to happen in the early summer. Thus shoots of almonds were harvested for evaluation of genotype heat tolerance at the peak of the PHSI in July of 2015. A total of 43 almond varieties were sampled with two outgroup reference species (pecan and walnuts). The almonds were divided into groups: i) *Nonpareil*, as a reference variety, measured at all sites, ii) 14 new commercial releases included in the Regional Variety Trial (RVT) at Chico (coded A1, A2…etc.), iii) 12 UC Davis breeding program entries in the Chico RVT, including varieties derived from crosses with other *Prunus* species (*P. persica*, *P. fenzliana*, *P. webbii*), iv) four USDA entries in the Chico RVT and v) 12 UC Davis breeding lines maintained at the Nickels Estate for Tom Gradziel.

Replicate shoots of almonds from the RVT trial and at Nickels were harvested on cool days (<90F) and returned to the lab at UC Davis. Leaf samples were processed as detailed in the Methods for Objective 1.

Work on variation in heat tolerance in ~30 *Prunus* species and ~20 more almonds varieties is underway and will involve work in August with John Preece and Carolyn DeBuse at the USDA GRIN resource at Winters.

*Acknowledgements:* Franz Niederholzer (UCCE Farm Advisor) is thanked for providing access to the Nickels almond breeding collection. Richard Rosecrance (CSU Chico) is thanked for

providing access to the Chico RVT trial. Furthermore the breeding work of Tom Gradziel (UC Davis) and Craig Ledbetter (USDA-ARS, Parlier) are essential, and greatly appreciated.

Objective 4. Evaluate tradeoffs of heat tolerance with other physiological processes
Please refer to Results and Discussion.

**Results and Discussion:**

Objective 1. Develop a protocol for high throughput measurement of leaf heat tolerance
A protocol based upon Schreiber and Berry (1977) was successfully developed and equipment built, and is a suitable screening tool for any future physiologist/breeder provided they have a suitable chlorophyll fluorometer. A description is given in the Methods and the protocol was used to achieve Objective 3.

Objective 2. What is the quantitative impact of high heat tolerance on leaf function?
The quantitative impact was evaluated in three manners, the results of which are detailed here.

*Objective 2a. Monitoring of almond heat stress*: **Figure 4** illustrates key results from experiments to determine how heat stress occurs. The figure shows the responses of three leaves to a day of severe water deficit, and the following day after rewatering. The parameter monitored is the efficiency of photosynthesis at photosystem II (PSII), which is termed maximal quantum efficiency of PSII ($F_v/F_m$) which only occurs at night time, and the quantum efficiency of PSII ($\phi_{PSII}$) which occurs during daylight. Any decrease of $F_v/F_m$ from 0.83 at night can be interpreted as the result of photosynthetic stress during the day. During the daylight, the differences in $\phi_{PSII}$ represent lowered photosynthesis, in this case, due to four days of soil water deficit.

The key points are that:
1) A high leaf temperature of 37$^o$C (97F) in the leaf, from the watered plant, under high light did not result in residual stress that night (leaf A; **Figure 4**),
2) A very high leaf temperature of 45$^o$C (113F) occurred in both the shaded leaf (B) and unshaded leaf (C) on the water stressed tree. The damage that night was much more severe in the unshaded leaf. **Thus it was the combination of soil water stress affecting stomata and thus photosynthesis AND the high light AND the high leaf temperature that led to photosynthetic stress.**
3) Reversal of the shades on the recovery day lead to greater recovery of the initially severely damaged leaf (C).

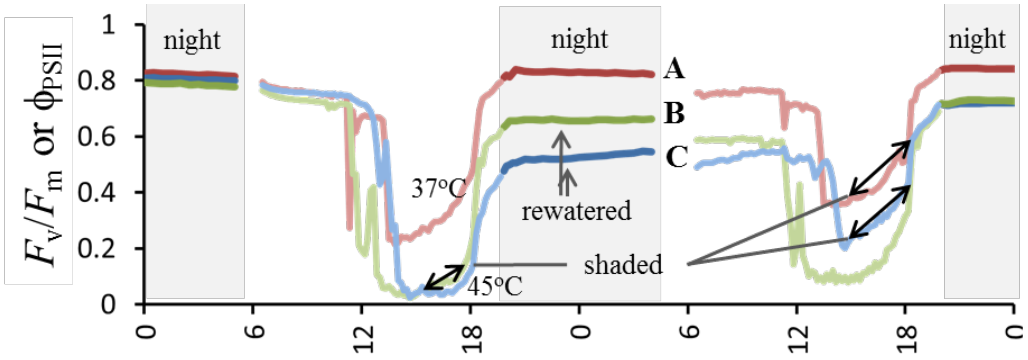


**Figure 4.** Interactions of heat, low stomatal conductance (water stress) and light on photoinhibition of PSII of almond leaves measured using the Walz MoniPAM. $F_v/F_m$ (nighttime) shows reversible photoinhibition, daytime values are quantum efficiencies ($\phi_{PSII}$). On day 1, water stress leads to stomatal closure of leaf B and C and high $T_{leaf}$ (45°C), while a well-watered control (A) has low $T_{leaf}$ (37°C). Shading (50%) leads to leaf B having less decrease in photosynthetic function than C. After re-watering and reversal of shading, C recovers more than B.

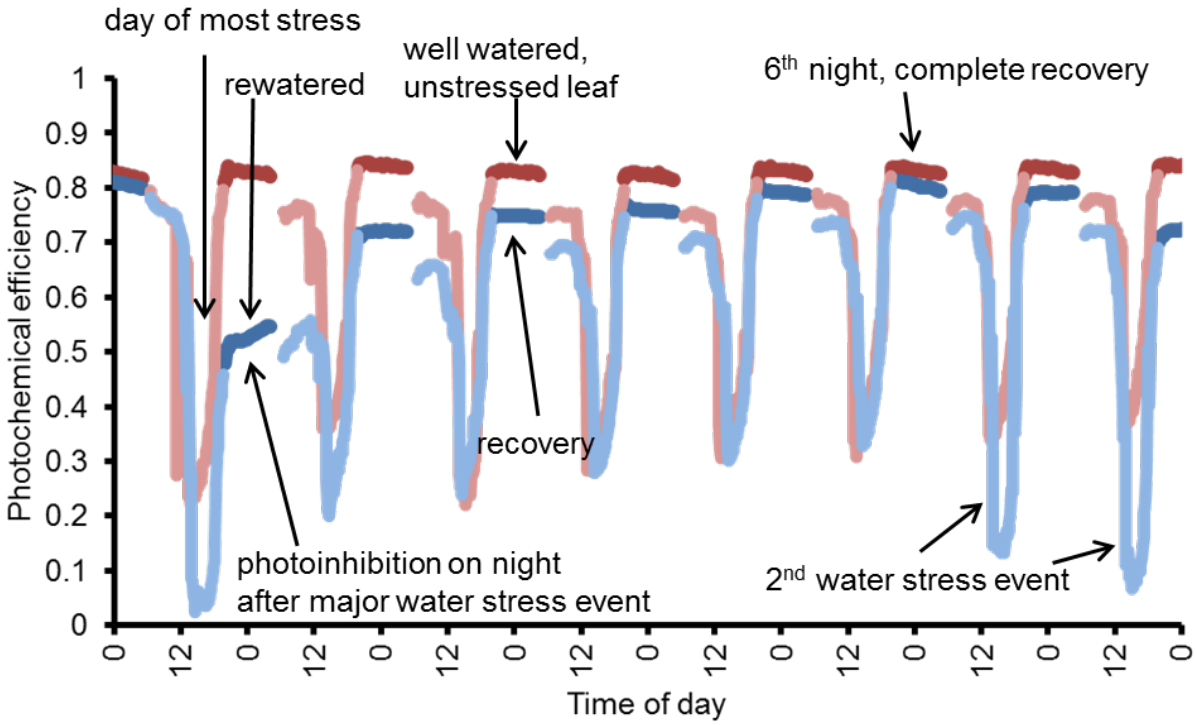


**Figure 5.** Eight days of recovery of two almond leaves after one was exposed to soil water deficit (high light and 45°C leaf temperatures) on the first day and rewatered that night. The data are the same as **Figure 3**, except expanded to demonstrate the entire recovery of the damaged leaf over six nights.

A combination of stresses led to a long term level of damage to the leaf photosynthesis apparatus, which showed surprising ability to recover (**Figure 5**). For instance, a leaf exposed to severe stress recovered control values by the sixth night of recovery. Thus severe water deficit, which occurs in California with the other factors leading to photosynthetic stress (high light and high temperatures), can result in long-term effects on photosynthesis, although almond shows remarkable ability to recover. Scaling these effects up to canopy level

performance is difficult, requiring either an eddy-covariance system to measure total orchard $CO_2$ exchange, or a modelling approach. We have proposed to address this scaling problem in the form of a National Science Foundation grant in which we propose to measure $CO_2$ exchange in almonds under stress and model the effect of photosynthetic damage.

The photosynthetic model discussed in Objective 2c was developed to address this scaling up problem, but is not at the developmental stage in which we can assess impacts quantitatively. However, it is expected that, based upon first principles, long term damage of PSII should lead to considerable decreases in photosynthetic performance. Our logic is: 1) decreases in $F_v/F_m$ (such as in **Figure 5**) typically scales proportionally with the parameters of the photosynthetic light response curve, but only sometimes affecting the maximal rates of photosynthesis (Long *et al.* 1994). If that is true, then at least light limited portions of the canopy would have limited photosynthesis under stress effects on PSII. Quantitatively this may lead to effects on photosynthesis of the same order of magnitude as the decrease in $F_v/F_m$ i.e. 40% for the duration of recovery. If light saturated portions of the canopy are also affected by stress on PSII, then the effects on photosynthesis may be greater.

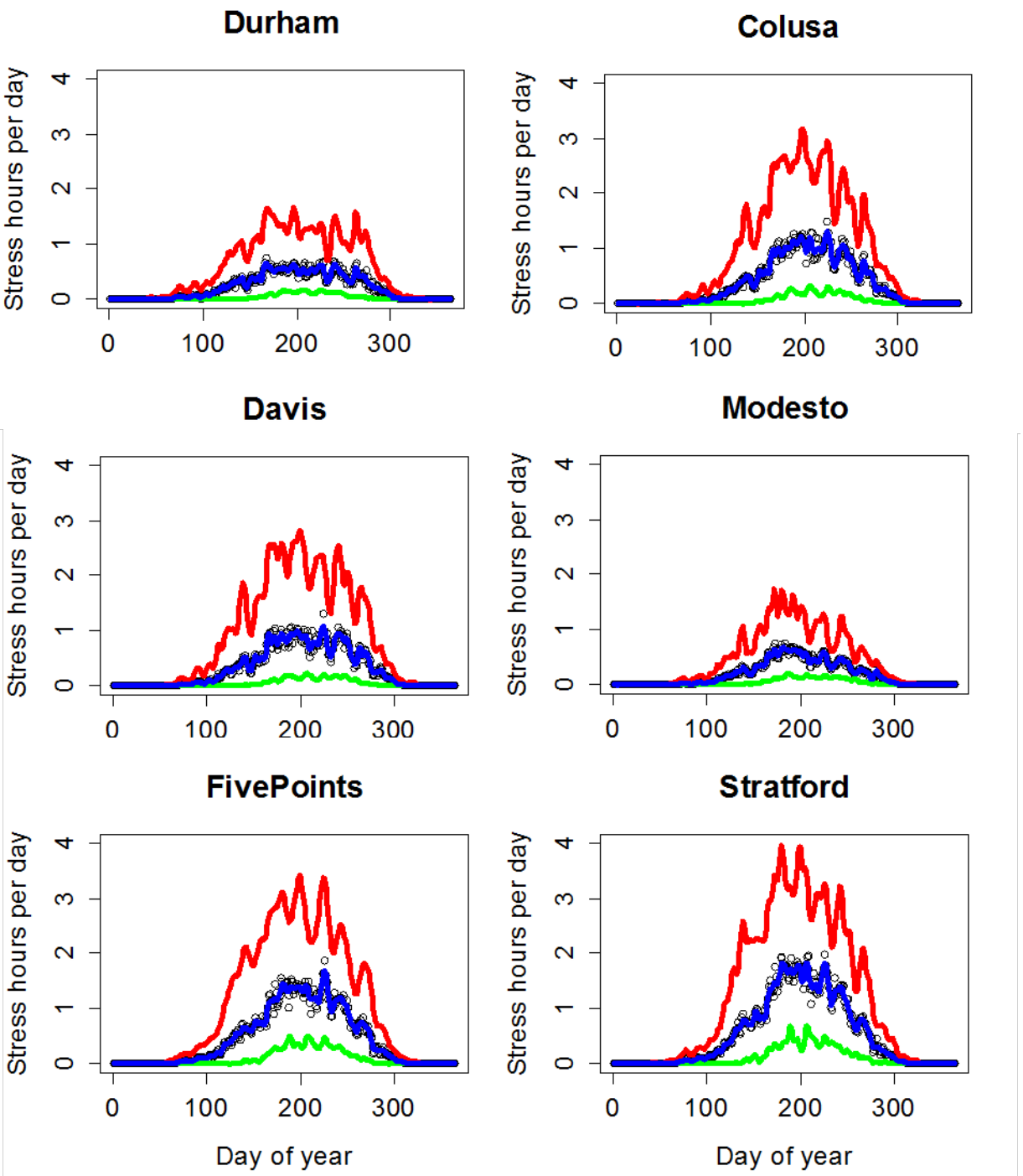


**Figure 6.** Results of modelling of the Potential Heat Stress Index (PHSI) for almonds with moderate to severe water deficit for twenty years of hourly weather data for six sites representative of almond growing regions in California. The points represent the daily number of hours of heat stress calculated using the PHSI detailed in the Methods. The black points represent the average PHSI for a day of the year, blue line the smoothed average, the upper red line the 19/20 or 95$^{th}$ percentile PHSI value for that day over the twenty years, and the lower green line the 1/20 or 5$^{th}$ percentile value.

*Objective 2b. Development of an index for heat stress*:
The Potential Heat Stress Index (PHSI) was applied to two northern Central Valley sites (Colusa and Durham), central sites (Davis and Modesto) and two southern Central Valley sites (Stratford and Five Points). The stress index is currently untested, in that it the prediction of stress has not been field tested at a range of sites. However it was developed based upon field data and serves well as a tool for evaluation of patterns of heat stress.

There is a clear trend to higher potential heat stress as one goes south in the Central Valley (**Figure 6**). This is expected as maximum temperatures increase with distance from the cooling effect of the San Francisco Bay. All sites had, in 95% of years, some degree of potential heat stress in the middle of the year, indicating that soil water deficit or salinity has the potential to lead to heat damage at all sites during June, July and August.

For all sites, April and May (day of the year ~100 to 150) had considerably lower PHSI values than the consistent high values for June, July and August (day of the year 150 onwards). This indicates that there is considerable time and heat signal for almonds to undergo acclimation responses to the increasing heat in more than the majority of years. Thus the existence of acclimation responses, or heat tolerance differences in leaves produced at different times of the year, would be an interesting future investigation.

A point of clarification is warranted: The PHSI is potential in the sense that it should only be interpreted as potential heat stress if almonds are under moderate to severe water stress. Without the leaf heating associated with stomatal closure under water stress, the heat stress index would be much lower. This can be evaluated by removing the solar radiation term in the $T_{air}$ index. Thus under well irrigated conditions heat stress effects on leaves will be low until extreme air temperatures are reached (>45C, 113F).

*Objective 2c. Development of a model of photosynthetic heat stress*:
The model of leaf heat stress response is detailed in the Appendix 1. It is currently undergoing further validation and testing. The future objectives of the model are to use it: i) to determine the impact of heat stress on the photosynthetic performance of almond canopies, ii) to integrate representations of stress in to the global climate models that are used to predict agricultural and vegetation response to shifting temperatures and climate. Once validated and published, the model will be available to any almond researcher/modeler, or before then on request.

<u>Objective 3. Rank the heat tolerance of almond genotypes and related species</u>
Heat tolerance was determined via the method developed in Objective 1. The critical leaf temperature represents the leaf temperature at which the key component of photosynthesis (PSII) starts being affected by high temperature. This effect is negative to leaf photosynthesis, but is recoverable.

While there is variation between varieties in heat tolerance (**Figure 7**), the variation is small (<4$^{o}$C) and the values are high. To put this in context, a study of canopy temperatures under drought stress found that on a 39$^{o}$C day (102F) almonds had ~34$^{o}$C canopy temperatures in the well watered treatment, and 41$^{o}$C temperatures in the severe drought treatment (Gonzalez-Dugo *et al.* 2012). For reference the severe drought treatment had water potentials of -2.5MPa or -25 bars. Therefore, only the canopy temperatures seen on the hot day and under drought

stress were high enough to be above the critical leaf temperature for damage to photosynthesis. Thus, in general, almonds operate at leaf temperatures lower than the threshold for damage. Thus the main conclusion is that all almonds are capable of considerable heat tolerance and that this is only important under water stress.

Further evaluation of **Figure 7** suggests that there may be variation between the temperature tolerances of varieties from different origins. An ANOVA comparing the four sources of almonds demonstrated that origin had a significant effect ($F_{3,38}$=3.69, p = 0.02). UC Davis breeding lines had the highest heat tolerance, followed by UC Davis entries in the RVT, then new commercial releases and the USDA entries in the RVT. However, it should be cautioned that the total variation in heat tolerance was small, the variance explained by the ANOVA was very low ($R^2$ = 0.23), the USDA had only four entries, limiting comparison, and varieties from any origin were found across the range of critical temperatures (**Figure 7**). **Thus our main conclusion is that there is little variation in heat tolerance amongst diverse advanced almond varieties.** The results also highlight that the use of other *Prunus* species (*P. persica*, *P. fenzliana*, *P. webbii*) for crossing in the UC Davis breeding program has not led to a decrease in heat tolerance. Indeed, the crosses may have led to a minor increase in heat tolerance.

Analysis of the heat tolerance of diverse *Prunus* species is underway and will allow determination of whether outside almond there is greater variation in heat tolerance. Initial indications are that almond has a very high heat tolerance relative to other crops, and relative to other *Prunus* species (**Figure 8**). These data are derived from an alternative method for measuring heat tolerance to the data of **Figure 7**, but illustrate that plum and peach appear to be slightly less heat tolerant than two varieties of almond. We thus conclude that almond appears to be well adapted to our climate, and it is only under severe water deficits or salinity, in combination with high temperature and high light that heat damage is likely to occur.

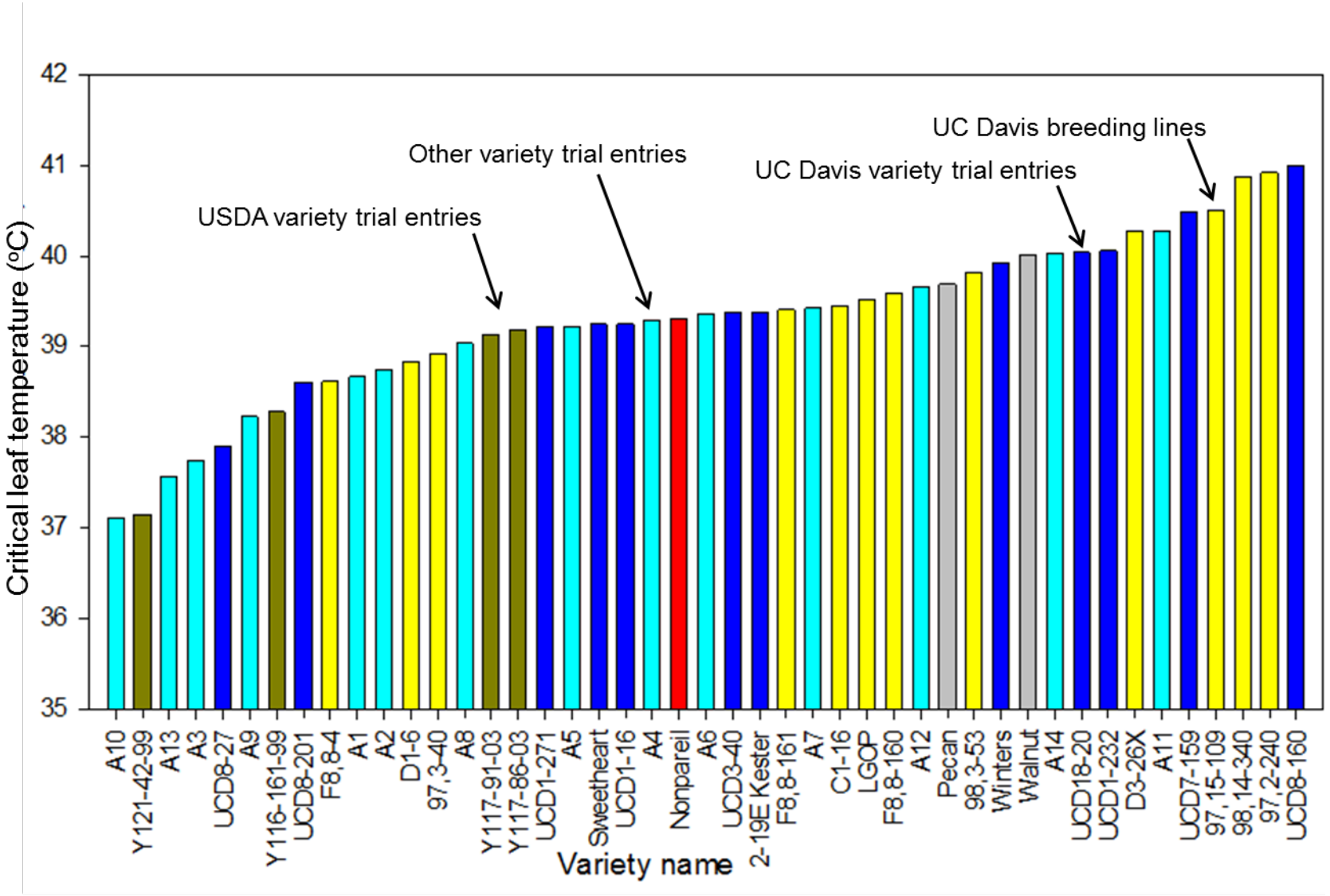


**Figure 7.** Variation in the critical leaf temperature for negative photosynthetic effects between 43 varieties of almonds from a number of sources. Nonpareil and pecan and walnut are included as references or comparison values. These data represent the results of fluorescence responses to temperature increases made on leaves, and described in the Methods, Objective 1. The almonds were harvested at the Regional Variety Trial at CSU Chico and orchards at Nickels Farm. 35°C = 95F and 42°C = 108F.

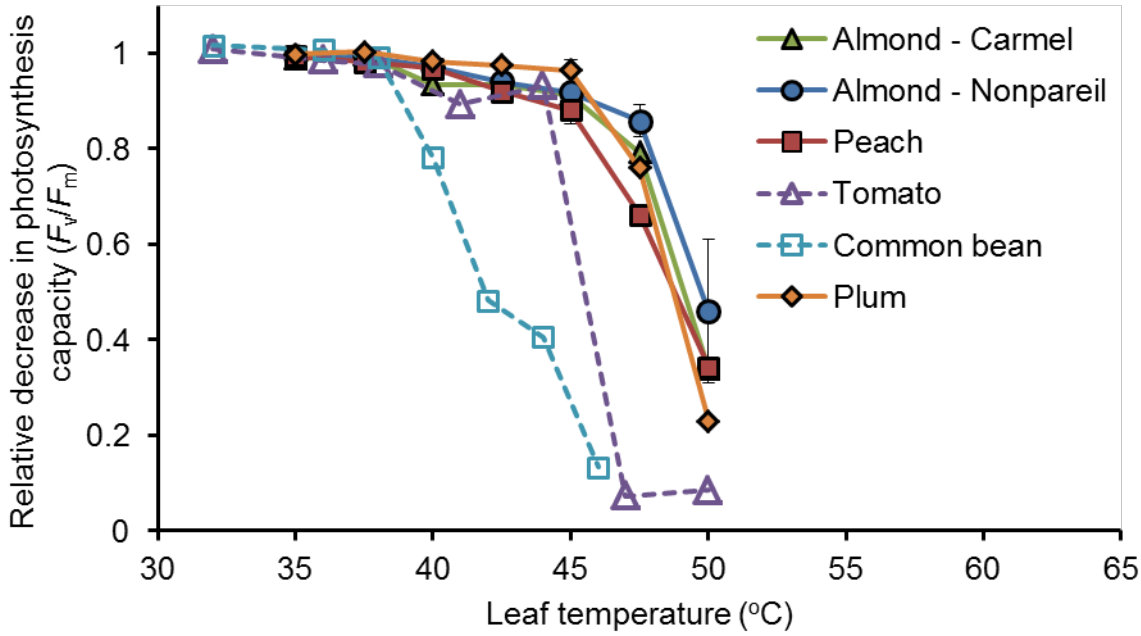


**Figure 8.** A comparison of absolute thermal tolerance of the leaf photosynthetic apparatus in *Prunus* species and two other crops. The decrease in the variable ($F_v/F_m$) signifies major, unrecoverable damage to the photosystem II.

Objective 4. Evaluate tradeoffs of heat tolerance with other physiological processes

A lack of variation in almond variety heat tolerance was found in Objective 3, and as a result there was no need to evaluate tradeoffs in that sample of almond varieties. However, it is anticipated that the more diverse *Prunus* germplasm to be sampled in August may have greater variation in heat tolerance and thus will allow an evaluation of tradeoffs.

**Research Effort Recent Publications:**

It is too early in the project to have published data, but two publications are envisaged in the following year: i) a ranking of the heat tolerance of almond genotypes and species and leaf physiological tradeoffs, ii) a model of almond heat tolerance physiology for inclusion in global climate models, structure-function models and used to assess the quantitative impact of heat tolerance on almonds.

**References Cited:**

Bernacchi C, Pimentel C, Long S (2003) In vivo temperature response functions of parameters required to model RuBP-limited photosynthesis. *Plant, Cell & Environment* **26**(9), 1419-1430.

Crafts-Brandner SJ, Salvucci ME (2000) Rubisco activase constrains the photosynthetic potential of leaves at high temperature and $CO_2$. *Proceedings of the National Academy of Sciences* **97**(24), 13430-13435.

Cunningham S, Read J (2006) Foliar temperature tolerance of temperate and tropical evergreen rain forest trees of Australia. *Tree Physiology* **26**(11), 1435-1443.

Gonzalez-Dugo V, Zarco-Tejada P, Berni JA, Suárez L, Goldhamer D, Fereres E (2012) Almond tree canopy temperature reveals intra-crown variability that is water stress-dependent. *Agricultural and Forest Meteorology* **154**, 156-165.

Jahns P, Holzwarth AR (2012) The role of the xanthophyll cycle and of lutein in photoprotection of photosystem II. *Biochimica et Biophysica Acta (BBA) - Bioenergetics* **1817**(1), 182-193.

Knight CA, Ackerly DD (2002) An ecological and evolutionary analysis of photosynthetic thermotolerance using the temperature-dependent increase in fluorescence. *Oecologia* **130**(4), 505-514.

Long S, Humphries S, Falkowski PG (1994) Photoinhibition of photosynthesis in nature. *Annual review of plant biology* **45**(1), 633-662.

Rosati A, Metcalf S, Buchner R, Fulton A, Lampinen B (2006) Physiological effects of kaolin applications in well-irrigated and water-stressed walnut and almond trees. *Annals of botany* **98**(1), 267-275.

Schreiber U, Berry JA (1977) Heat-induced changes of chlorophyll fluorescence in intact leaves correlated with damage of the photosynthetic apparatus. *Planta* **136**(3), 233-238.

## Appendix 1: Description of a photosynthetic model of almond induction and recovery from heat, light and water stress

*In the course of the experiments described in the main report, a detailed model of almond photosynthesis recovery from combined stresses was proposed, and has been partially validated. For completeness the model is presented here, but it is technical and insufficient explanation is provided for a lay audience, hence the separation into the appendix.*

The net photosynthetic rate ($A_n$) of a leaf is typically modelled as a function of two key processes that may be damaged by stresses: RuBP-regeneration ($A_j$) and Rubisco limited photosynthesis ($A_c$) minus the day respiration ($R_d$):

$$A_n = \min(A_c, A_j) - R_d \qquad \text{eqn. 1.}$$

We propose that parameters that determine $A_c$ and $A_j$ are dynamically affected by damage, photoinhibition or long term adjustments, and propose the following formulation to account for damage.

*Rubisco limited photosynthesis*
$A_c$ is represented through an equation that holds just one parameter – the maximum carboxylation rate ($V_{cmax}$) – that is typically varied in photosynthetic modelling. The other parameters are considered conserved, although have inherent temperature responses ($\Gamma_*$, $K_c$ and $K_o$). The remaining symbols, $C_c$ and O, are variables:

$$A_c = \frac{V_{cmax}(C_c - \Gamma_*)}{C_c + K_c(1 + O/K_O)} \qquad \text{eqn. 2.}$$

Typically $V_{cmax}$ is represented as responding to temperature by a humped distribution, such as an Arrhenius plot, where initial kinetic responses exponentially increase $V_{cmax}$ to about 35 to 40$^o$C, whereupon deactivation responses occur. However deactivation or damage to Rubisco are dynamic processes, although the reactivation time may be short. Thus, $V_{cmax}$ is adequately represented by a single increasing Arrhenius function, and activation and/or damage are represented by a dynamic component of the base $V_{cmax}$ value ($V_{cmax25oC}$). Thus,

$$V_{cmax} = V_{cmax25\ ^oC} * e^{-A_{Vcmax}/(T_{leaf}R)} \qquad \text{eqn. 3.}$$

where $A_{Vcmax}$ is an empirical constant, $R$ the gas constant, and,

$$V_{cmax25\ ^oC} = k_{ccat}\left(E_{act,t} - damage - recovery\ rate\right) \quad \text{eqn. 4.}$$

where, $E_{act,t} \geq 0\ \&\ E_{act,t} \leq E_{act,opt}$.

Equation 4 is defined similarly to Rubisco activation, but would include dynamic components.

*Rubisco damage:* it remains unclear how Rubisco is limited by high temperatures. Rubisco actives is thought to limit the pool of activated Rubisco ($E_{act}$) at high temperature (Crafts-Brandner *et al.* 2000), but recovery may be rapid enough (minutes) to treat it as an instantaneous recovery (dynamics in eqn. 4 are unnecessary for most $T_{leaf}$ values due to Rubisco having rapid recovery <<10min). Rubisco denaturation would result in more long term

damage to $V_{cmax}$ and $E_{act}$ (at very high $T_{leaf}$ denaturation would occur leading to long term dynamics in Rubisco content), but its presence needs to be empirically determined. The formulation to represent Rubisco would include one or more dynamic processes and use a form of the dynamic equation proposed for NPQ (eqn. 9). Stressful temperatures directly affect Rubisco, so it is unnecessary include damage by light or water stress.

*Photoinhibition and damage in modelling RuBP-regeneration*

$A_j$ is limited by light, or the electron transport rate for a given $T_{leaf}$ ($J_{Tleaf}$) and set of environmental conditions. Thus,

$$A_c = \frac{J_{Tleaf}(C_c - \Gamma_*)}{4C_c + 8\Gamma_*} \qquad \text{eqn. 5.}$$

$J_{Tleaf}$ is a non-rectangular hyperbolic function of a number of parameters that are temperature responsive (Bernacchi *et al.* 2003) and are affected by photoinhibition and PSII damage:

$$J_{T_{leaf}} = \frac{I_2 + J_{max} - \sqrt{(I_2 - J_{max})^2 - 4\theta I_2 J_{max}}}{2\theta} \qquad \text{eqn. 6.}$$

where,

$$I_2 = PPFD * abs * \phi_{PSII,max} * \beta \qquad \text{eqn. 7.}$$

Each parameter ($J_{max}$, $\phi_{PSII,max}$, $\theta$, $\beta$, abs) could be modeled as a positive function of temperature, as determined experimentally (increasing Arrhenius functions, eqn. 3, represent parameter response to temperature once photoinhibition effects are removed). Most parameters scale with the maximum photochemical efficiency of PSII in the dark ($F_v/F_m$) (Long *et al.* 1994) and thus we propose, and will test, $F_v/F_m$ is a key scaling parameter linking photoinhibition and light responses.

Damage due to reactive oxygen species (ROS) and photoinhibition due to long term up-regulation of non-photochemical quenching may be simply modelled, as each factor that dissipates energy absorbed by PSII ($W_{abs}$) and adjusts relative to already modelled photosynthetic responses to environmental variables (water deficit, $T_{leaf}$, PPFD). Thus,

$$W_{abs} = W_{excess} + W_{fluorescence} + W_{qE} + W_{qZ} + W_{qI} + W_{photochemistry} \qquad \text{eqn. 8.}$$

where each component has photon units ($\mu$mol $m^{-2}$ $s^{-1}$) and is described below:

- $W_{abs}$ is the total absorbed PPFD by PSII (=absorbance*0.5*PPFD).
- $W_{excess}$ is a function of the remainder of the energy not dissipated with the other sinks, and will be tested as the trigger of programmed cell death and bleaching of chlorophyll and loss of absorbance.
- $W_{fluorescence}$ is a small component that will not be modelled, but is included for completeness.
- The NPQ quenching components are $q_E$, $q_Z$ and $q_I$; sensu Jahns & Holzwarth (2012), are

modelled as fluxes:
  - o $W_{qE}$ is a very rapid PsBs and lumen pH dynamic component of NPQ.
  - o $W_{qZ}$ is a rapid dynamic component of NPQ (< day).
  - o $W_{qI}$ is a slow occurring dynamic component of NPQ that relates to a number of processes that inactivate, damage and affect photochemistry.
- $W_{photochemistry}$ is a function of the photosynthetic fluxes and flux of energy to photorespiration and other sinks such as nitrate assimilation. Modelled via eqn. 1 plus flux to photorespiration.

We propose that $W_{abs}$, and components, affect RuBP-regeneration through a coupling factor: $F_v/F_m$ which responds to components of NPQ. $F_v/F_m$ is modelled as a linear function of the long-term $W_{qI}$ component of NPQ, consistent with the literature. Note that unlike other model approaches; here water stress effects on photosynthesis are indirect and interactive with other environmental variables (it is adequate to represent stress as a function of the above equations, without the need to incorporate direct effects of cell water status on photosynthetic physiology).

Time dependent components of PSII non-photochemical quenching are modelled with a novel continuous, not discrete, function of time:

$$W_{x,capacity,t} = W_{x,capacity,t-\rho} + \frac{W_{x,attractor,t} - W_{x,capacity,t-\rho}}{1+{}^{\tau_x}/_{\rho}} \qquad \text{eqn. 9.}$$

Where $W_{x,capacity,t}$ and $W_{x,capacity,t-\square}$is the generic capacity of *x* quenching component (μmol $m^{-2}$ $s^{-1}$) at time *t* or the previous time (*t*-$\rho$; $\rho$ is the time interval between modelled points, set at 1 minute to be as fast as the most rapid NPQ components). The time constant for ($\tau_x$) each quenching component could be the same for increases or decreases. The dynamic equation includes the $W_{x,attractor,t}$ that sets the value that $W_{x,capacity,t}$ is drawn to. For rapid dynamic components, $W_{qE}$ and $W_{qZ}$, the attractor would be the excess absorbed photons assuming no NPQ, while for slow component, $W_{qI}$, the attractor would be the excess energy from the previous time point. These equations produce a capacity for NPQ, which could be higher than the actual flux. Thus the fluxes are adjusted from the capacities via the ratio of $W_{excess,no\ NPQ}/W_{NPQ\ capacity}$ (absorbed photons are assigned to potential photochemistry first and then the remainder is assigned to each NPQ flux equally). The NPQ fluxes require bounding parameters including zero and empirically determined maximum capacities.

Components of RuBP-limitation, $J_{max}$, $\beta$, and $\phi_{PSII,max}$, are affected by photoinhibition and some show a linear relation with $F_v/F_m$. $F_v/F_m$ as a coupling factor in turn affects the RuBP-regeneration parameters through the general proportionality which will be tested:

$$a_x = a_{max} \frac{F_v/F_m}{F_v/F_{m\,max}} \qquad \text{eqn. 10.}$$

Where $a_x$ is the parameter (e.g. $\phi_{PSII,max}$), $a_{max}$ is the maximum value for the parameter, and $F_v/F_m$ and $F_v/F_{m,max}$ the actual and maximum value of the coupling factor.

Model evaluation

The model as described above is functional, and can be used to predict reasonable photosynthetic dynamics (e.g. **Appendix Figure 1**). If standard photosynthetic parameter values are used along with widely published temperature corrections, and approximate values for the NPQ modelling are added, then the effect of low $F_v/F_m$ on photosynthesis can be calculated. **Figure 3** shows such modelling for a leaf undergoing one day of drought stress and a recovery day. The model demonstrates that the quantitative effect of NPQ on $F_v/F_m$ and on photochemistry is largely dependent on the time constants for the slow NPQ component ($W_{ql}$). Equal time constants for increases and decreases in $W_{ql}$ (e.g. 6 hours) result in little effect on cumulative photosynthesis for a drought period of 3 days followed by 4 recovery days. But as can be seen in the empirical data from the main report, $F_v/F_m$ takes days to increase to unstressed levels, but dropped in one day. Thus $W_{ql}$ decreases are likely of the order 7 days, while increases are rapid (*vice versa* for $F_v/F_m$). **In this relatively realistic case, the cumulative effect of photoinhibition on photosynthesis is a decrease of 35% during the period of stress and recovery.**

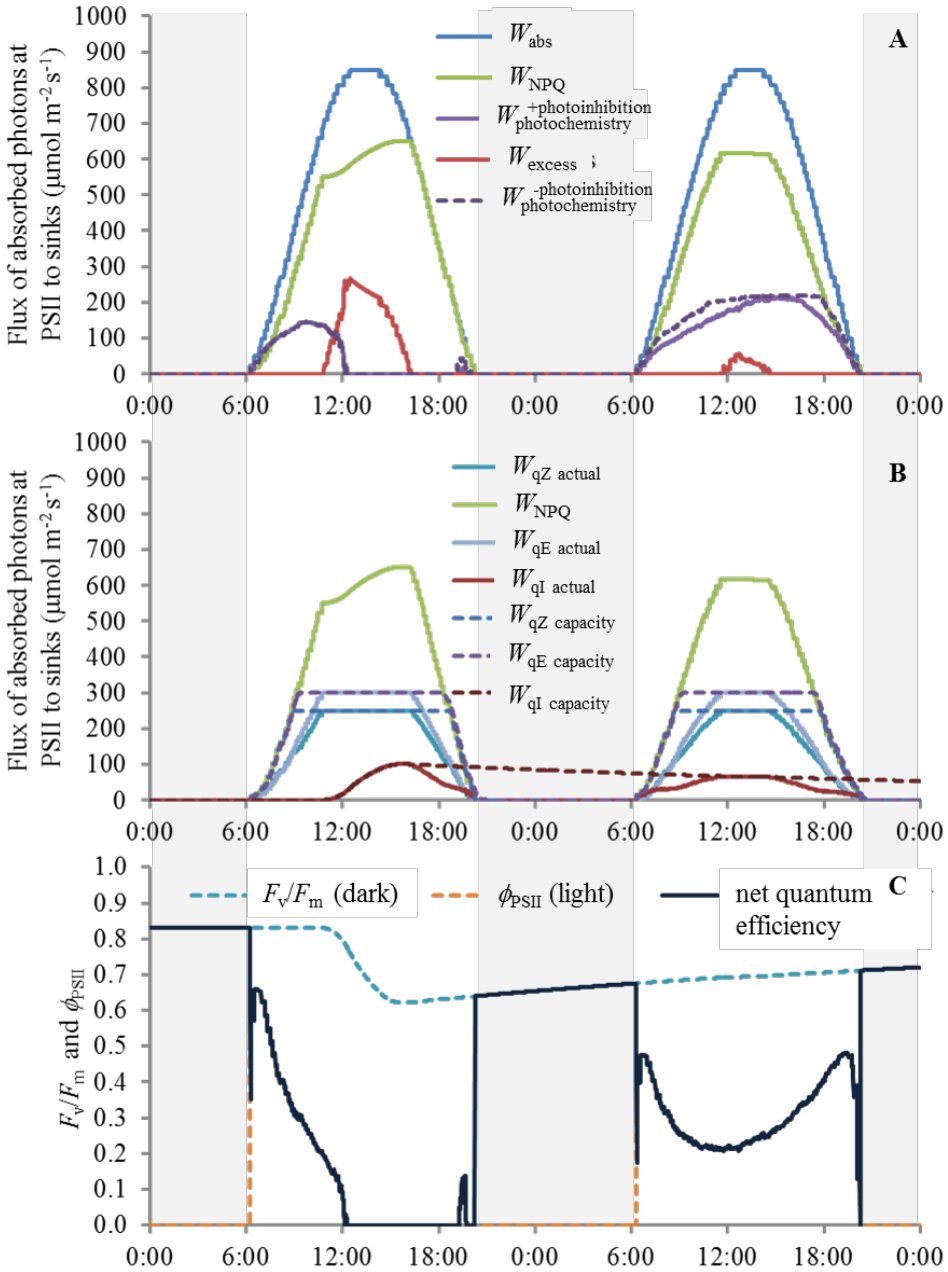


**Appendix Figure 1.** Simulated sinks of absorbed PPFD by PSII (panel A), fluxes and capacities of the three modelled components of NPQ (panel B), and effects on $F_v/F_m$ and $\phi_{PSII}$ of photoinhibition (panel C) for a leaf exposed to severe stomatal closure on the first day, and rewatering by the second. For illustrative purposes the modelled $F_v/F_m$ is shown for daytime, and the flux to photochemistry is shown for leaves with and without photoinhibition effects (all other data represent photo inhibited leaves). The slow NPQ component ($W_{qI}$) had time constants of 6 hrs and 2 d for the increases and decreases, respectively. These data were modelled using the equations proposed above, but without negative Rubisco effects.